INTERNATIONAL JOURNAL OF RESEARCH IN AERONAUTICAL AND MECHANICAL ENGINEERING

ISSN (ONLINE): 2321-3051

Vol.3 Issue.1,

January 2015.

Pgs: 88-98

A REVIEW PAPER OF PARAMETRIC ANALYSIS AND RESEARCH DIRECTIONS IN WIND TURBINE BLADES

TUKESH THAKUR

PG SCHOLAR (DEPARTMENT OF MECHANICAL ENGINEERING, MATS UNIVERSITY, RAIPUR)

Abstract

This review paper describe the problems associated with adverse aerodynamic loads will grow more critical. Electricity production from wind energy has grown at a fast pace over the last few years. The size of individual wind turbines has also increased significantly and it is unclear if this trend can b sustained in the future for structural reasons, especially regarding rotor blade components. A research programme is being undertaken to investigate these issues, and finite element modelling will be extensively used to examine the static and dynamic limitations of wind turbine blades. As an initial step in this research, a flexible full blade model was created and is presented in this

paper. The wind energy technical community has begun to seriously consider the potential of aerodynamic control methodologies for mitigating adverse aerodynamic loading. Spatial and temporal attributes of the structures and processes present in these flow fields hold important implications for active aerodynamic control methodologies currently being contemplated for wind turbine applications. The current work uses complementary experimental and computational methodologies, to isolate and characterize key attributes of blade flow fields associated with axisymmetric and yawed turbine operation. During axisymmetric operation, a highly three-dimensional, shear layer dominated flow field yields rotational augmentation of both mean and standard deviation levels of aerodynamic forces.

Keywords – Wind Turbine Blades, Process Automation, blade variables.

1. Introduction

The energy problem we are facing today is articulated around two main drivers: supply and greenhouse gas emissions. Renewable energy sources are an inevitable part of the solution, and wind energy is, at the moment, the fastest growing installed production technology. Commercial wind turbines have developed consistently in size over the last thirty years, largely for economic reasons in an attempt to reduce the electricity production cost, typically measured in p/kW.h. This is due to the fact that wind speed – and hence wind power capture – increases with altitude and that reducing the number of individual turbine units helps to reduce the overall cost of a wind farm, especially offshore. As shown in Figure 1, the largest current machine has a rated output of 5 MW and a rotor diameter of 124 m and so the question arises as to what the ultimate limits on size might be. In all cases, wind turbine blades have pure strength requirements. A static case can, for instance, be calculated on the basis of a 50-year return period gust, while fatigue strength for a 25-year lifetime implies cycle numbers of the order of 107. Another crucial requirement relates to the blade stiffness, since at all times a minimum

clearance must be ensured between the blade tip and the turbine tower. The increase in diameter also makes the rotor and blade mass related requirements more severe. Not only do the blade root and the rotor hub need to sustain the static loads (the 62m world-largest blade weighs ~18T), but the nacelle structure, tower and foundations also need to sustain the whole machine dynamics. For a complete discussion of design requirements, interested readers can refer to Burton *et al.* (Burton, 2001).

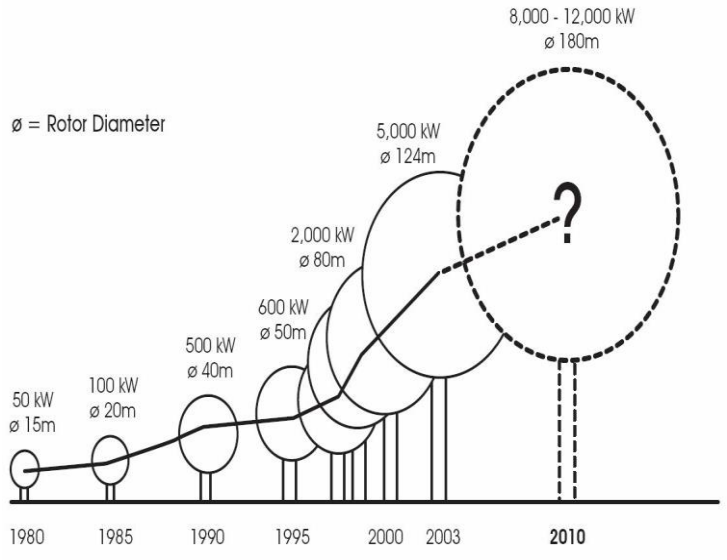

Figure 1. Wind turbine size development (source: European Commission, 2005)

Wind turbine aerodynamics remains a challenging and crucial research area for wind energy. Clearly, steady-state aerodynamic performance is essential to turbine energy capture, since blade aerodynamic forces produce mechanical energy that is subsequently converted to electrical energy. However, more recent inquiry has focused on adverse time varying aerodynamic loads that wind turbines frequently suffer during routine service. These undesirable aerodynamic loads impose excessive stresses on turbine blades and gear boxes, and appreciably shorten machine service life. At present, the wind energy technical community is contemplating the utility of various aerodynamic control methodologies for mitigating adverse aerodynamic loading.

Wind turbine blade aerodynamic phenomena can be broadly categorized according to the operating state of the machine, and two particular aerodynamic phenomena assume crucial importance. At zero and low rotor yaw angles, rotational augmentation determines blade aerodynamic response. At moderate to high yaw angles, dynamic stall dominates blade aerodynamics. As described herein, the spatial and temporal attributes of the structures and processes present

Parametric blade model strategy development

- **Generic blade topology**

Although the aerodynamic surfaces can be complex because based on non-planar surfaces, complete blade geometry can be defined by way of a fairly simple topology adequate with our goal of obtaining a parametric model. It is based on the definition of 2D shells for the aerodynamic surfaces and the internal shear-web composites and 3D bricks for volumes of glue used to connect the sub-components. As shown in Figure 2, the outer shape can merely be defined by consecutive sections (e.g. circle at the root and specific aerofoil profiles)

and a list of distances from root to tip where each section is present. The aerodynamic shape can then be finally defined by an interpolation process creating a smooth surface through the successive curves.

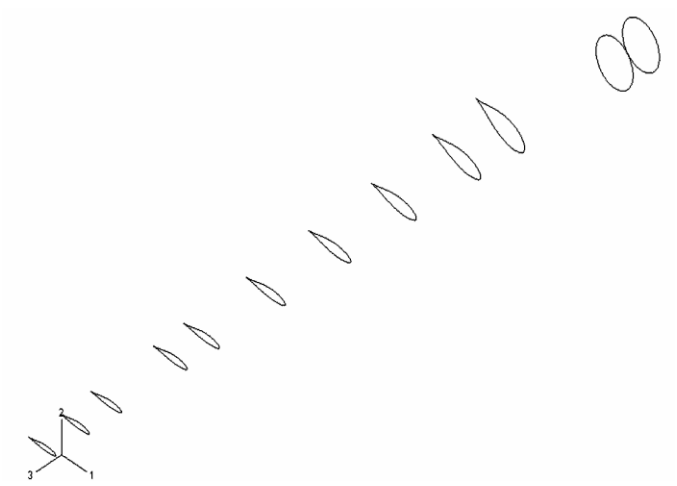

Figure 2. Outer shell topology.

Similarly, the internal structure, typically shear webs, can be parametrically defined by stipulating the distances from root where they start and end as well as the transverse ratios (defined as percentage of chord length) where they will connect to the outer skins. Finally, a glue layer can be inserted between shear-webs and skins, defined by its thickness. The shear-webs and glue volumes can be seen in Figure 3. In this topology, it should be noted that the shear-webs may not necessarily start and end at places defined by aerofoil sections. Similarly, the various regions that receive specific composite layups may not be defined according to the longitudinal split of the blade defined by the aerofoil sections. Finally, even though Figure 2 shows a particular type of shear-web shape, only minor modifications should be needed to the model to reflect other types (e.g. I beam or closed square section). The model adopted should respect these independencies. Because of the nature of our research project, a fully parameterised and extremely flexible modelling strategy is aimed at, so that the blade external geometry, internal structural shape, materials used, loading, analysis type and post-processing operations can be adjusted independently. In turn, the model development time will be optimised and a massive proportion of the Abaqus usage time will be spent producing the results. These specifications lead to the use of a Python script as the analysis definition core. All aspects of an analysis process can be automated in the script, and the full features of the Python programming language confer numerous options for parameterisation.

Examples of parametric analysis

To illustrate the modelling strategy adopted, four parametric analyses are presented below. For each of these studies, once the sweep is set-up and the script execution started, no more user interaction is necessary to produce or compile the complete set of results presented. In these analyses, the blades are simply loaded at the tip in the direction of the wind, which is also the most critical loading direction given the section orientation of a wind turbine blade. The results presented do not constitute significant advances in wind turbine blade engineering.

- **Mesh convergence analysis**

A typical but necessary optimisation problem when conducting FEA work is that of the mesh resolution convergence. How refined does the mesh need to be? How many degrees of freedom can be solved in the time frame available? A mesh convergence analysis was conducted on a typical blade model. Five meshes of increasing resolution were produced. The meshes are shown in Figure 3 as viewed from the root, looking inside the blade – note that this view point means that
the mesh elements mostly look stretched, even though they have in fact good proportions.

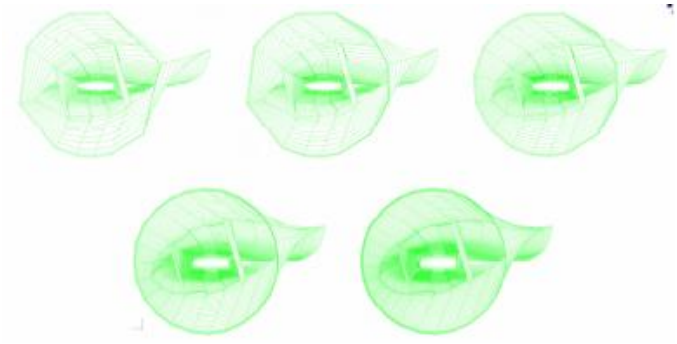

Figure 3. Meshes obtained in mesh size sweep analysis.

These meshes were analysed consecutively and the results presented in Figure 4 were obtained. With the smallest 0.03 m mesh size parameter, the mesh refinement process has converged for general stiffness analyses, as shown by the slope of the tip deflection curve on figure 4. This mesh will be used in the following sections.

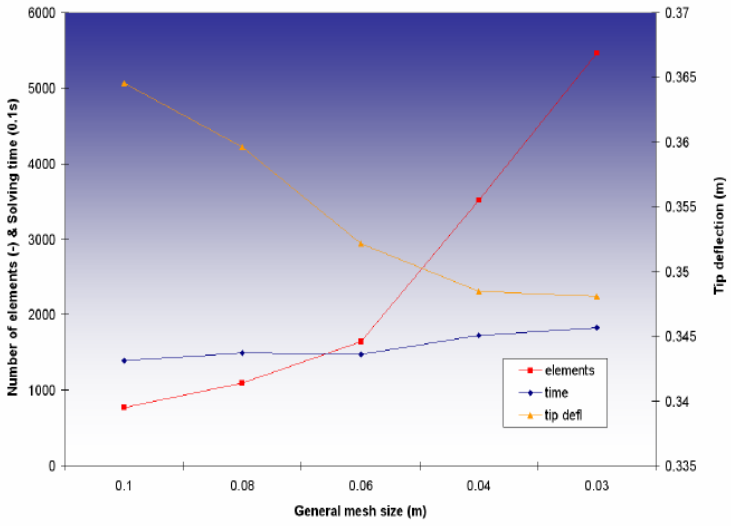

Figure 4. Mesh size sweep results.

- **Shear-web transverse placement**

The transverse placement of the shear-webs within the aerofoil sections naturally influences the structural properties of the assembly. Due to the twist angle variations along the blade, a bending loading state always

introduces torsion in some sections of the blade. Such torsion modifies the angle of attack of the aerodynamic surfaces, in turn causing a modification in loading – such a phenomenon is generally described as aero-elastic. The influence of the shear-web placement on the blade mass, bending stiffness and bending-torsion coupling is studied in this example. Six different geometries are examined as shown in Figure 5. In each one, the shear-webs are moved in opposite directions, from being very close to each other to being near the leading and trailing edges. The various geometries are analysed and the results are presented in Figure 6. Note that, as the shear-web spacing increases, the blade mass grows significantly. This is because in the particular layup used, the composite stack applied in the outer skin in-between the two shear-webs is significantly heavier than that applied near the leading and trailing edges. In terms of blade stiffness, it is found that the increase in shear-web spacing also brings higher stiffness values, both in terms of linear and angular displacements. Although the analysis results presented here are valid, they raise the question of cross-coupling between the various design parameters, and it emerges that parameter sweeps with cross coupling of several independent parameters would be necessary in this case. Alternatively, and perhaps more comprehensively, optimization graphs could be produced from the script where iso-parameter contours can be interpolated, improving the understanding of the interdependency between various design parameters.

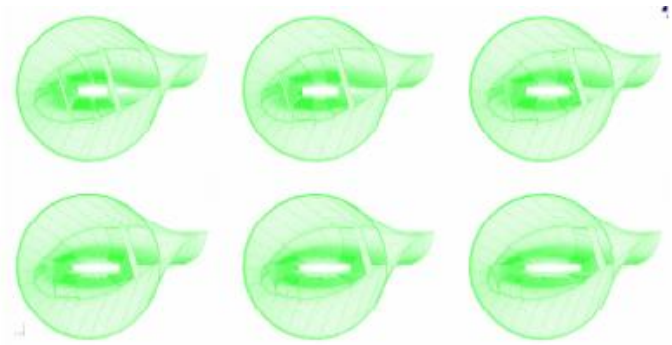

Figure 5. Meshes obtained in shear-web transverse placement analysis.

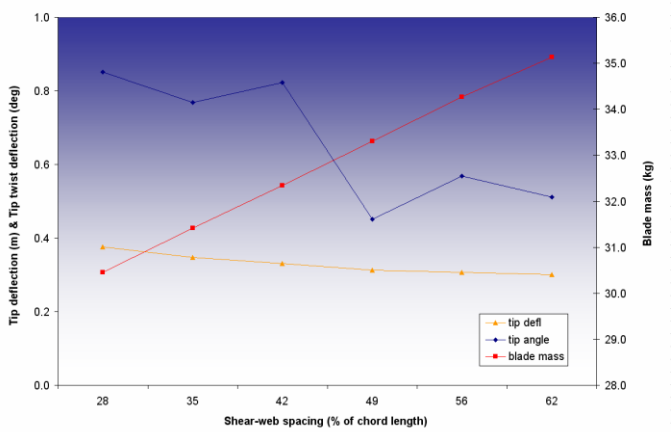

Figure 6. Shear-web placement sweep results.

- **Aerofoil shape**

The parametric blade geometry definition also enables a study into the effect of the aerofoil shape on the structural properties of the finished component. Here, we have compared the baseline model used so far with two variations that use different profile series: the Wortmann FX84W and

the Althaus AH93W (see Selig, 2006 for full coordinate listing). The blade produced with the Wortmann aerofoils uses a round root section, while a specific root profile, wider but a lot thinner, is provided in the Althaus aerofoil series – note that such a profile would bring significant construction constraints in the case of a pitch operated blade. The aerofoil coordinates are contained in plain text files (one file for each blade section), referred to from within the Python script. Figure 7 shows the meshes obtained for the three aerofoil types. These meshes show once again the validity of the mathematical geometry and mesh generation and its adaptability to substantially different designs.

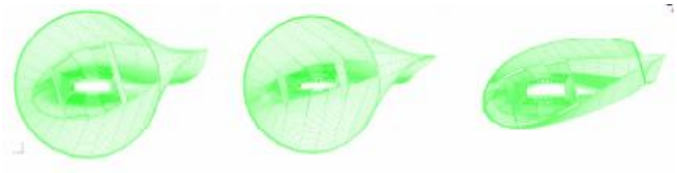

Figure 7. Meshes obtained with three different aerofoil series.

The static analysis results obtained for the three aerofoil series are displayed in Figure 8. It can be seen that a change from the baseline aerofoils to the Wortmann series, all other parameters constant, would be beneficial in terms of blade mass but detrimental in terms of stiffness. A change for the Althaus series seems very beneficial in mass terms and only a little detrimental in terms of stiffness. These results variations are mostly due to the relatively stiff and heavy sections near the root and the maximum chord area – the Wortmann series has a significantly thinner maximum chord profile while the root section of the Althaus blade has a much smaller circumference, but is still stiff enough compared to the rest of the blade, perhaps providing a better compromise.

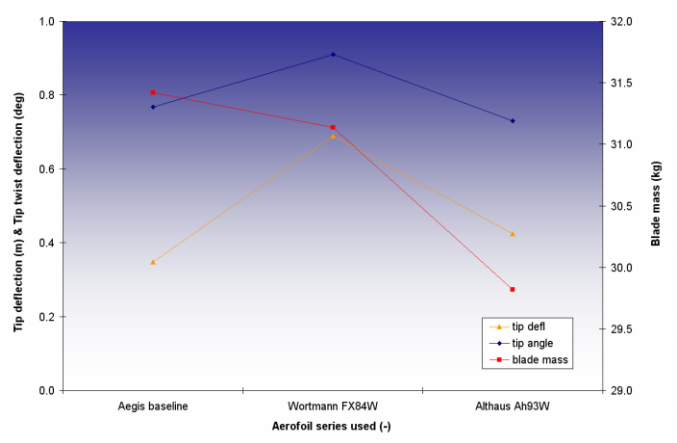

Figure 8. Aerofoil series sweep results.

Rotational Augmentation

Augmentation of rotating blade aerodynamic properties, including stall delay and lift enhancement, was first observed for airplane propellers and qualitatively explained in terms of centrifugal and Coriolis accelerations.[1] Some time later, analytical modeling quantitatively accounted for key elements of the rotating blade flow field.[2]

Subsequent rotational augmentation research was carried out for helicopter rotors. Analytical modeling determined that rotationally induced cross flows played an important role in blade lift production.[3] Experimental research [4] suggested that centrifugal forces are important in the presence of flow separation, but of limited influence otherwise.

Prior research concerning rotational augmentation of airplane propeller and helicopter rotor aerodynamics aided later work aimed at wind turbines. However, wind turbines extract energy from flowing air, while propellers and rotors inject energy. This key distinction pointed out the need for rotational augmentation research specific to wind turbines.

Early wind turbine field testing aimed at rotational augmentation affirmed the importance of blade geometry with respect to rotational influences.[5] A wind tunnel experiment showed that blade geometry coupled with blade rotation maintained blade lift under conditions in which lift otherwise would significantly decline.[6] Subsequent wind tunnel research determined that rotational augmentation was most active at the inboard portion of the turbine blade.[7] Concurrent analytical modeling of rotational augmentation has furnished better comprehension of the aerodynamics underlying this phenomenon, and provided foundational predictive capabilities for design and analysis.[8-13]

More recently, analysis of turbine aerodynamics measurements acquired during controlled wind tunnel experiments, in conjunction with validated computational results, have provided key physical insights regarding rotationally augmented flow fields. [14-17]

2. EXPERIMENTAL PROCEDURES

All surface pressure data used in the current work were acquired during wind tunnel testing of the NREL UAE (National Renewable Energy Laboratory Unsteady Aerodynamics Experiment) horizontal axis wind turbine. This machine was documented in detail for earlier field testing phases of the experiment. Subsequently, several UAE configurations were tested in the NASA Ames 80 ft x 120 ft wind tunnel, all of which are described by Hand, et al.

Wind Turbine

Data analyzed in the current work were acquired from a two bladed upwind rotor, 10.1 m in diameter, with zero cone angle. The rotor turned counterclockwise (viewed from upwind) at a constant 71.6 RPM, was stall regulated, and had a maximum rated power of 19.8 kW. A cylindrical tower 0.4 m in diameter supported the turbine at a hub height of 12.2 m (test section centerline), with 1.32 m rotor overhang. This UAE configuration is depicted in Figure 10.

Figure 10. NREL Unsteady Aerodynamics Experiment wind turbine in NASA Ames 80 ft x 120 ft wind tunnel.

Blade Geometry

The blades used throughout the NASA Ames wind tunnel test were both twisted and tapered. Blade taper distribution is apparent in Figure 11, with chord tapering from 0.737 m at 0.25R to 0.356 m at the tip. Blade section twist decreased from 22.1° at 0.25R to 0.0° at the tip. Between 0.25R and the tip, blade cross-section was uniform, corresponding to the S809 airfoil. The airfoil section at 0.25R was joined to the pitch shaft section at 0.12R using linear segments to yield an uninterrupted transition between these two disparate contours. The blade pitched about an axis located 0.30c aft of the leading edge, and centered between the blade upper and lower surfaces at that chord location. Design procedures, constraints, and measures of merit for this blade have been documented in detail.

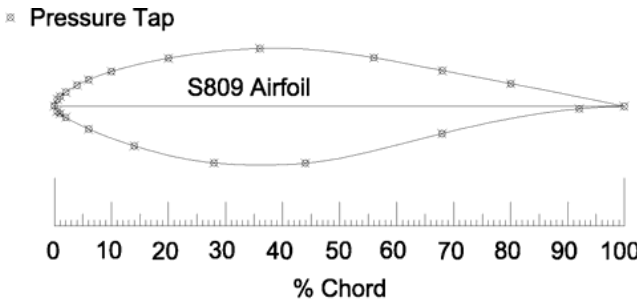

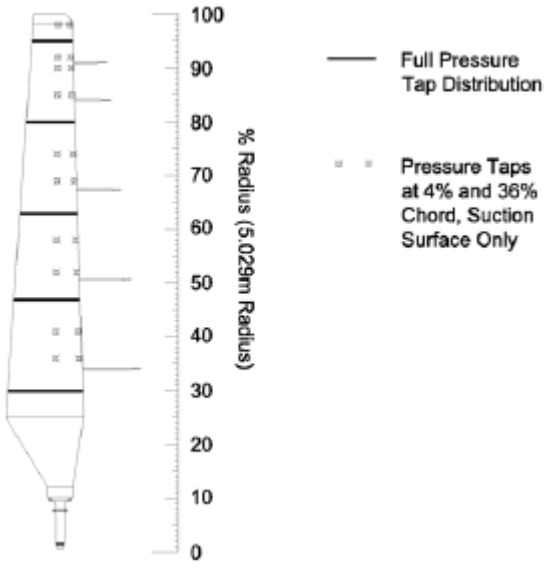

Figure 11. Blade cross-section and planform, showing pressure tap locations.

Data Acquisition Protocol

Data acquisition procedures were designed to decouple the principal physical phenomena that govern blade aerodynamics, and thus were structured in an incremental manner. First, blade aerodynamics was characterized for nonrotating conditions. Then, data were acquired with the blades rotating at zero yaw, for a range of wind speeds. Finally, with the rotor still turning, yawed conditions were characterized for a matrix of wind speeds and yaw angles.

To isolate the effects of rotational influences, a baseline was needed that excluded rotational effects. This was accomplished by halting turbine blade rotation and acquiring pressure data for the stationary (parked) blade. To achieve stationary blade conditions, the instrumented turbine blade was first fixed at the 12 o'clock azimuth position. Then, for $U\infty$ = 20 m/s, turbine blade pitch was incremented in 5° steps, from 90° to -15° and -15° to 90°. Blade pitch was incremented in both negative and positive directions to disclose any hysteresis in blade aerodynamic force response. At each pitch angle, one 13 second data record was acquired, and cp data from each record were integrated over the sectional chord to obtain time records of Cn. Finally, these 13 second time records of cp and Cn were time averaged to yield mean values for each blade pitch angle. Prior to acquiring data at each pitch angle, appropriate delays were included to allow time for pitching, blade flow field equilibration, and wake relaxation.

To quantify the effects of rotational influences, data were collected with the rotor turning at 71.6 RPM. Turbine blade plane of rotation was maintained orthogonal to the test section centerline, yielding $\gamma = 0°$. Blade pitch angle was held constant at 3.0°. $U\infty$ was varied between 5 m/s and 25 m/s, in nominal 1 m/s increments. At each $U\infty$, a data record of 30 seconds duration was acquired, corresponding to 36 blade rotations.

Inflow Angle and Force Nondimensionalization

Derivation of angle of attack and lift coefficient for rotating blades using measurements on or near the blade remains a challenging and essential area of inquiry. However, in the current work, these dependencies were

excluded in order to simplify physical relationships and concentrate analyses on the blade flow field. This was accomplished by analyzing measured LFA and Cn in lieu of derived α and Cl.

Normalization of aerodynamic forces also presents challenges. In the current work, normal force was nondimensionalized by local dynamic pressure. Local dynamic pressure was computed as the difference between test section static pressure (p∞) and local total pressure. Local total pressure was sensed at each full pressure tap distribution as the highest pressure in the tap distribution. This methodology for quantifying dynamic pressure has been analyzed previously, and found to induce average errors in dynamic pressure of approximately 1.0 percent.

3. RESULTS AND DISCUSSIONS

Results and discussion below are divided according to turbine operating state into two sections, axisymmetric operation and yawed operation. As summarized above, these two operating states produced flow fields dominated by rotational augmentation and by dynamic stall, respectively. Within each of these two sections, results and discussion follow the same progression. First, inflow relationships are described. Then, typical data for mean and standard deviation of normal force are presented.

4. Future developments

The future work in this research will be articulated over three main drivers. First, the blade model described in this paper needs to be developed with known and potential improvements. The blade loading, as described above, will be fully parameterised and implemented within the blade model script. This will imply that the aerofoil performance data is accessed from external files produced by the panel code tool. Later, this can be developed into an aero-elastic analysis tool by creating a feedback loop from the calculated blade deflections at various sections to the generation of an updated load field. At this stage, fully dynamic blade analyses can be conducted and the structural dynamics of whole wind turbine machines be investigated. Also, the main composite mesh elements, currently described by 2D shells, would perhaps more accurately be modelled by 3D continuum shells. This investigation will involve a comprehensive model calibration, which can be conducted at two levels:

• On a sub-component level, in collaboration with materials research specialists within our Supergen consortium, bespoke tests of manufactured components will be carried out and reproduced computationally.

• On the whole blade level, full blade certification test data from our industrial partner collaborators will also enable crucial model validation and calibration. And of course substantial work will be devoted in parallel to address the project questions regarding future generations of wind turbines. The current blade technology will first be replicated and potential improvements will be investigated. To this end, the material data such that collected in the Optimat Blades Project (Knowledge Centre Wind Turbine Materials and Constructions , 2006), in which the second author was an active partner, will be an invaluable knowledge source.

5. CONCLUSION

Using complementary experimental and computational methodologies, key attributes of blade flow fields were isolated and characterized for axisymmetric and yawed turbine operation. These characteristics are likely to have strong implications for control of turbine blade flow fields.

For axisymmetric operation, elevated inflow angles drive Cn to mean and standard deviation levels that are significantly augmented relative to two-dimensional non-rotating conditions. Both mean and standard deviation levels are substantial, and are caused by a highly three-dimensional, shear layer dominated flow field.

In this paper, a generic model was presented to generate and analyse the structural behaviour of large composite wind turbine blades. The model is programmed in the analysis process is entirely automated and parameterised. Typical potential applications to wind turbine blade structural engineering issues were presented and the model showed good coherence and extreme adaptability. Special considerations were then presented regarding the generation of accurate aerodynamic loading procedures, and future developments of the model and of the current research were described.

6. REFERENCES

[1] Bechly, M. E., and P. D. Clausen, "Structural Design of a Composite Wind Turbine Blade Using Finite Element Analysis," Computers & Structures, vol. 63, pp. 639-646, 1997.

[2] Burton, T., D. Sharpe, N. Jenkins, and E. Bossanyi, "Wind Energy Handbook," John Wiley & Sons Ltd, 2001.

[3] de Goeij, W. C., M. J. L. van Tooren, and A. Beukers, "Implementation of bending-torsion coupling in the design of a wind turbine rotor blade," Applied Energy, vol. 63, pp. 191-207, 1999.

[4] McCroskey, W. J., "Measurements of Boundary Layer Transition, Separation and Streamline Direction on Rotating Blades," NASA TN D-6321, Apr. 1971.

[5] Madsen, H., and H. Christensen, "On the Relative Importance of Rotational, Unsteady and Three-Dimensional Effects on the HAWT Rotor Aerodynamics*," Wind Engineering*, v. 14, n. 6, 1990, pp. 405-415.

[6] Ronsten, G., "Static Pressure Measurements on a Rotating and a Non-Rotating 2.375 m Wind Turbine Blade. Comparison with 2D Calculations," *J. of Wind Engineering and Industrial Aerodynamics*, v. 39, 1992, pp. 105-118.

[7] Corten, G., "Inviscid Stall Model," Proceedings of the European Wind Energy Conference, July 2001, pp. 466-469.

[8] Schreck, S., and Robinson, M., "Rotational Augmentation of Horizontal Axis Wind Turbine Blade Aerodynamic Response," *Wind Energy*, v. 5, n. 2/3, pp. 133-150, Apr.-Sep. 2002.

[9] Shipley, D., M. Miller, and M. Robinson, "Dynamic Stall Occurrence on a Horizontal Axis Wind Turbine Blade," NREL/TP-442-6912, Jul. 1995. Golden, CO: National Renewable Energy Laboratory.

[10] Robinson, M., R. Galbraith, D. Shipley, and M. Miller, "Unsteady Aerodynamics of Wind Turbines," AIAA 95-0526, 33rd Aerospace Sciences Meeting and Exhibit, Jan 1995.